

# Hierarchical Condensation

Xiao Yan,<sup>†</sup> Feng Chen,<sup>\*,‡</sup> Soumyadip Sett,<sup>†</sup> Shreyas Chavan,<sup>†</sup> Hang Li,<sup>†</sup> Lezhou Feng,<sup>†</sup> Longnan Li,<sup>†</sup> Fulong Zhao,<sup>‡</sup> Chongyan Zhao,<sup>‡</sup> Zhiyong Huang,<sup>‡</sup> and Nenad Miljkovic<sup>\*,†,§,||,⊥</sup>

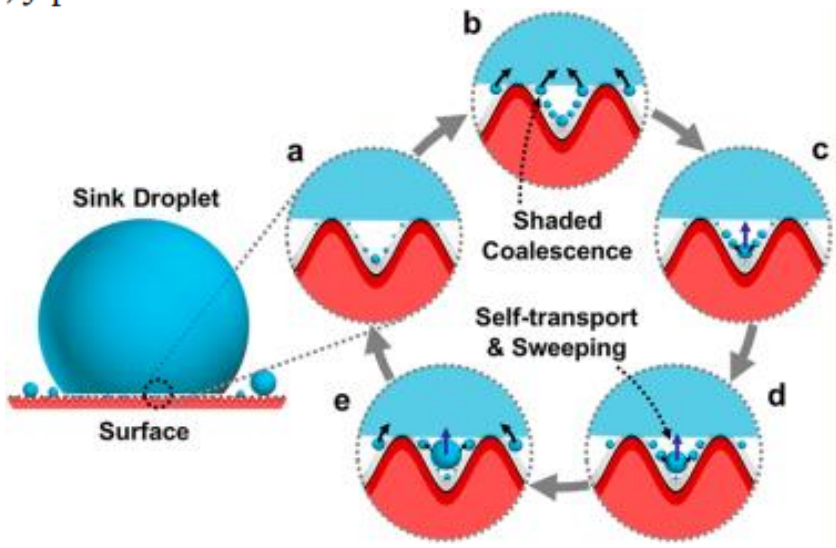
<sup>†</sup>Department of Mechanical Science and Engineering, University of Illinois at Urbana–Champaign, Urbana, Illinois 61801, United States

<sup>‡</sup>Institute of Nuclear and New Energy Technology, Tsinghua University, Beijing 100084, China

<sup>§</sup>Department of Electrical and Computer Engineering, University of Illinois at Urbana–Champaign, Urbana, Illinois 61801, United States

<sup>||</sup>Frederick Seitz Materials Research Laboratory, University of Illinois at Urbana–Champaign, Urbana, Illinois 61801, United States

<sup>⊥</sup>International Institute for Carbon Neutral Energy Research (WPI-I2CNER), Kyushu University, 744 Moto-oka, Nishi-ku, Fukuoka 819-0395, Japan



Paper presentation

1<sup>st</sup> Group meeting

04-01-2020

Ankit Nagar

# Background

- Condensation heat transfer has potential to enhance the efficiency of thermoelectric power generation, high heat flux thermal management, and water distillation
- The efficient removal of condensate is key to improving heat transfer due to the condensate becoming thermal-conduction-limited at larger length scales
- Utilizing surface chemistry to transition the condensate morphology from a thin film to discrete droplets has been shown to enhance heat transfer by 10X.
- Dropwise condensation: gravity-assisted shedding, sweeping of the surface, and time-averaged droplet size
- Minimum droplet departure size= 500 nm (viscous forces, surface adhesion)

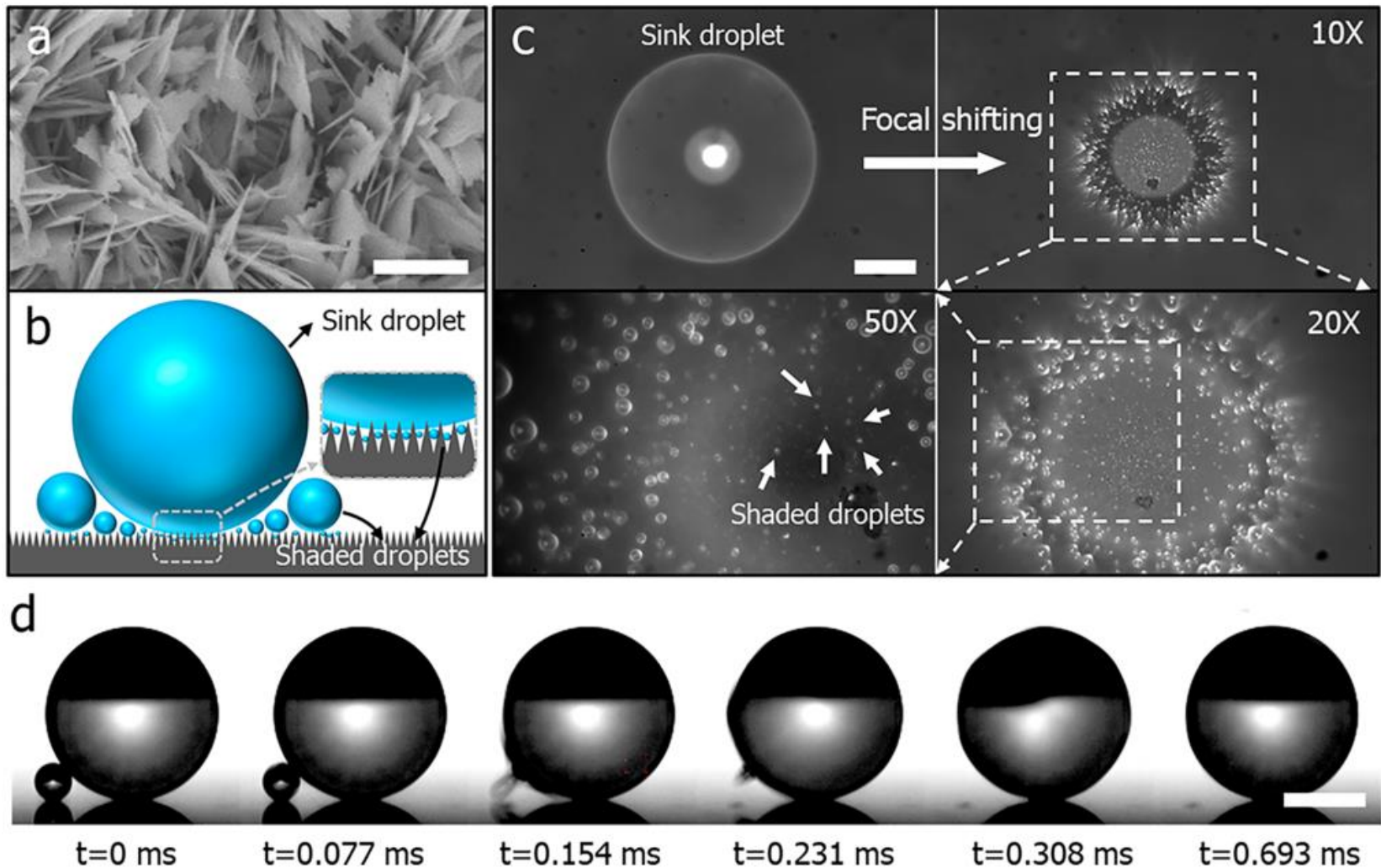
## **Relevance:**

Water harvesting, self-cleaning surfaces

# Introduction

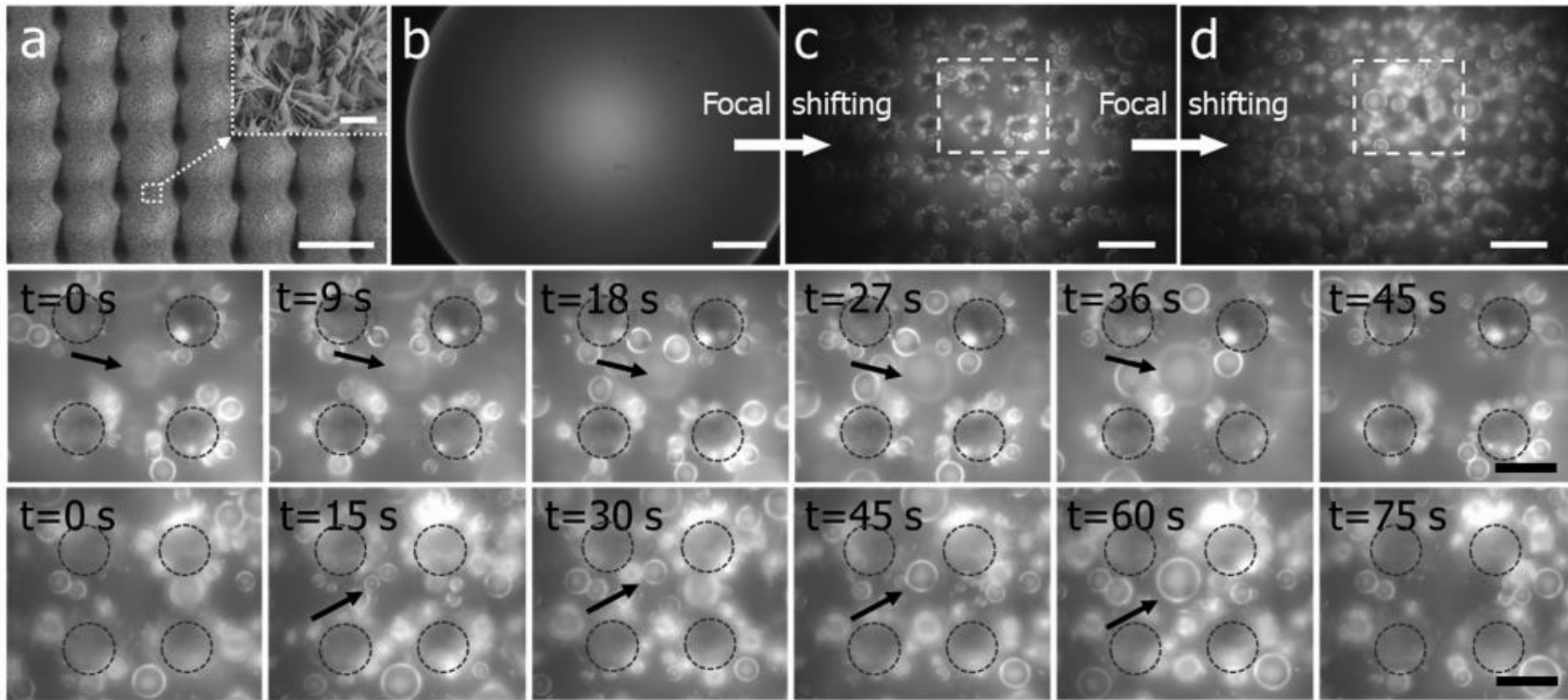
- An efficient approach of shedding micro- and nanoscale condensate droplets without the need for jumping
- A removal mechanism equivalent to droplet jumping that relies only on classical gravitational shedding and enables greater durability
- Hierarchical surfaces consisting of copper-based hill-like microstructures ( $\sim 10\ \mu\text{m}$ ) with conformally coated copper oxide (CuO) nanoblades ( $\sim 1\ \mu\text{m}$ )

# Sink droplets and shaded coalescence



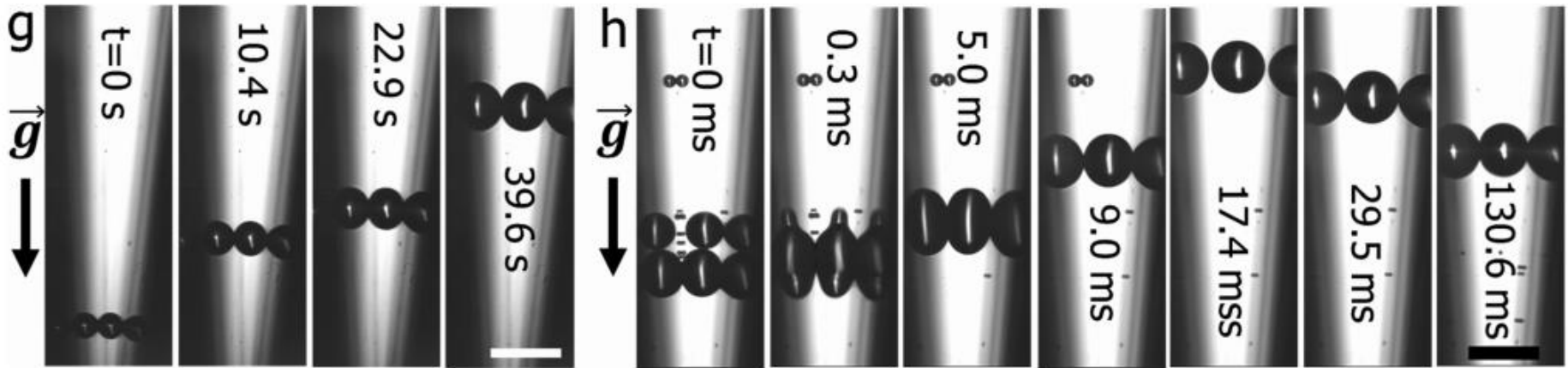
SEM of the superhydrophobic single-tier CuO nanoblade surface. Scale bar: 1  $\mu\text{m}$ . (b) Schematic of shaded coalescence. (c) Top-view high-speed optical microscopy showing small shaded droplets surrounding and beneath a large sink CB droplet. The focal plane in the second (10 $\times$ ), third (50 $\times$ ), and fourth (20 $\times$ ) images is located at the droplet base. Scale bar: 200  $\mu\text{m}$ . (d) Side-view high-speed time lapse images showing the coalescence dynamics of a sink droplet (diameter:  $218 \pm 1.0 \mu\text{m}$ ) and a smaller shaded satellite droplet (diameter:  $48 \pm 0.5 \mu\text{m}$ ). Scale bar: 200  $\mu\text{m}$ .

# Hierarchical condensation



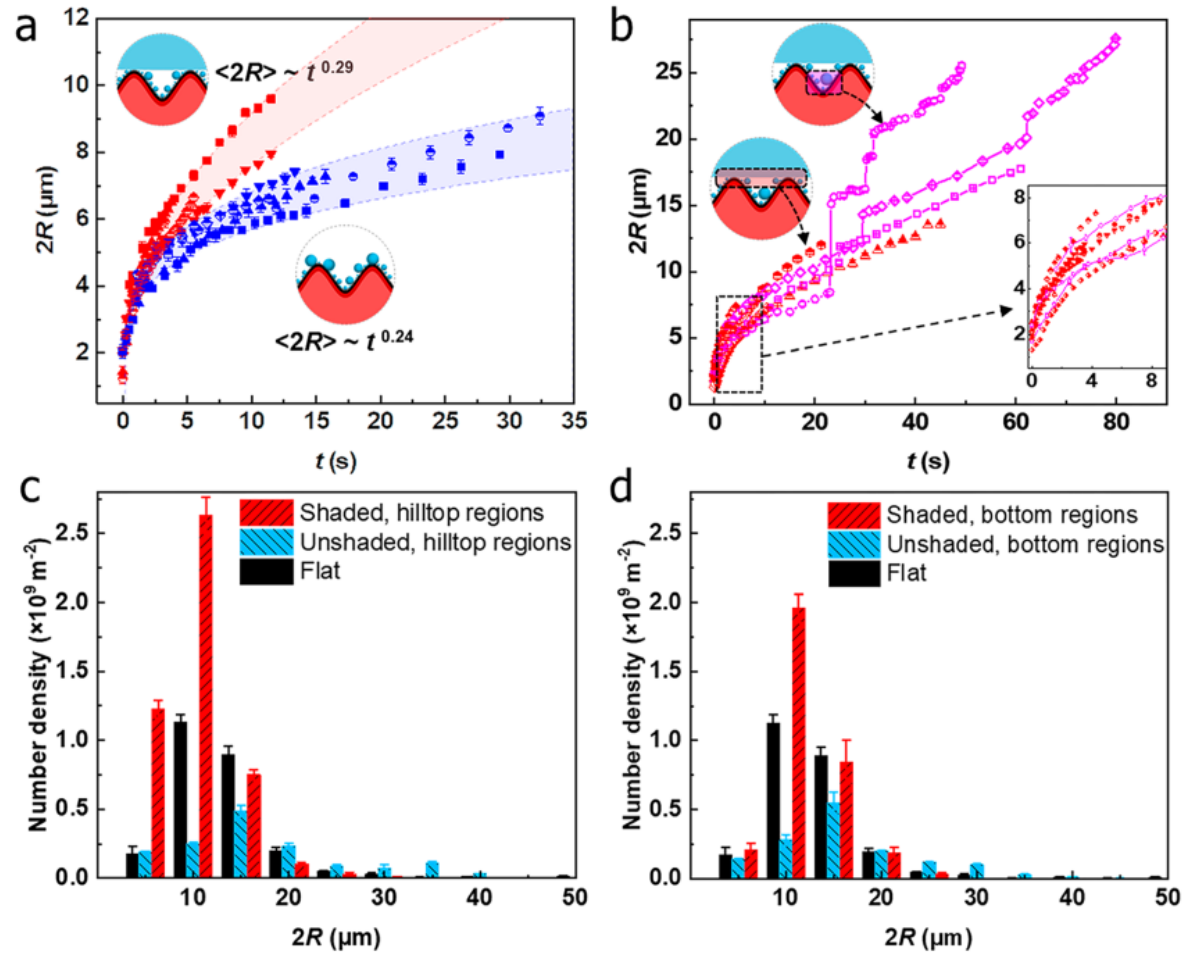
(a) SEM image of the hierarchical CuO nanoblade surface. Scale bar: 50  $\mu\text{m}$ . Inset: High-resolution SEM of the surface in (a). Scale bar: 1  $\mu\text{m}$ . By shifting the focal plane of the optical microscope toward the sample, we observed (b) the sink droplet, scale bar: 100  $\mu\text{m}$ , and (c and d) small droplets within structure cavities, scale bars: 20  $\mu\text{m}$ . Microscopy images showing growing droplets at a focal plane (c) beneath the sink droplet and (d) 20  $\mu\text{m}$  lower than the focal plane in (c). (e and f) Time lapse images of droplets growing beneath the sink droplet corresponding to the white dotted sections in (c) and (d), respectively. Black dotted circles trace the microstructure features. The black arrows in (e) trace the growing droplets navigating upward in the cavity due to the passive Laplace pressure-driven motion. Scale bar: 20  $\mu\text{m}$ . (f) Time lapse images showing frequent coalescence between underlying droplets prior to shaded coalescence with the sink droplet. Scale bar: 20  $\mu\text{m}$ . The black arrows in (f) trace the coalescence events at the bottom region of the cavity.

# Hierarchical condensation



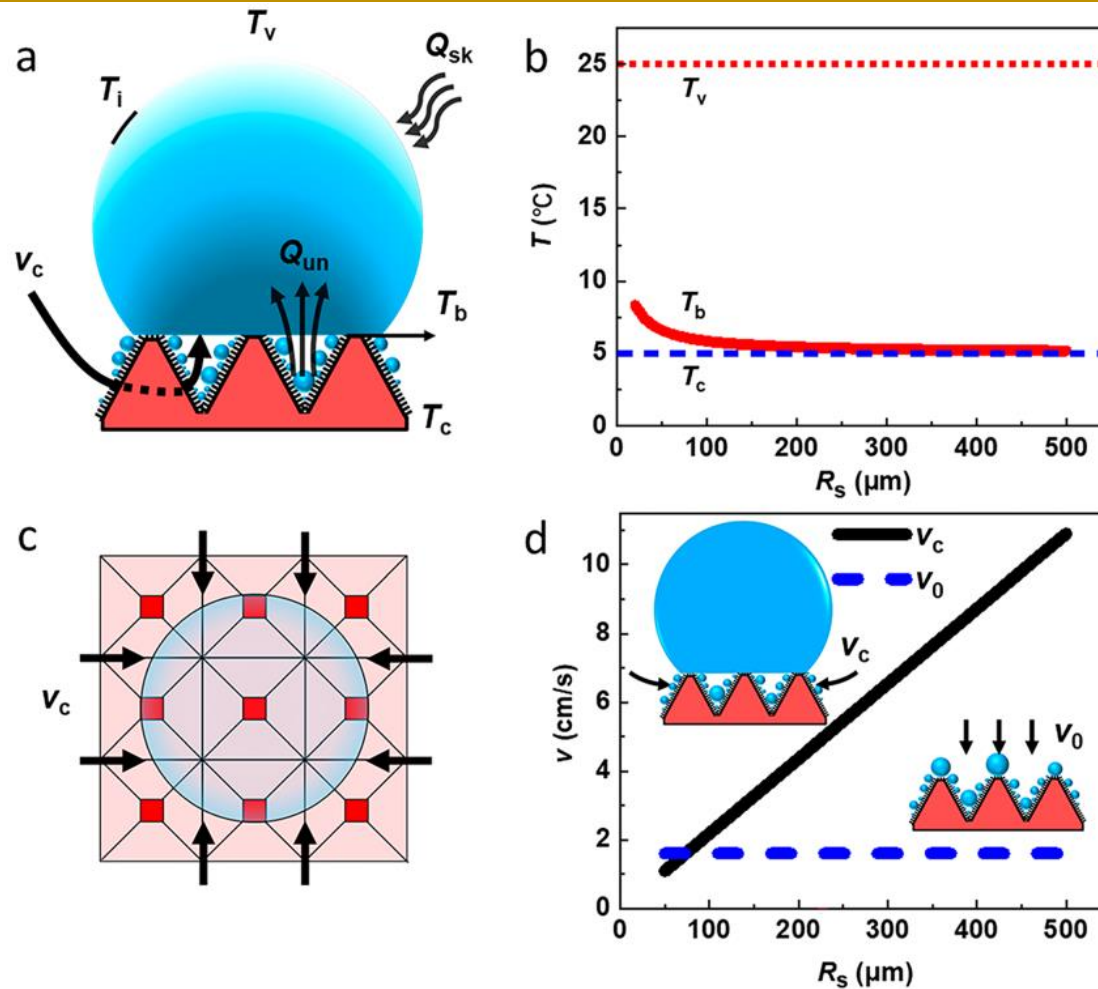
Experimental demonstration of upward transport of (g) a growing droplet and (h) two coalescing droplets residing in a groove with an opening angle of  $5.3^\circ$ . Scale bars:  $500 \mu\text{m}$ .

# Enhanced droplet growth and nucleation rate of shaded droplets



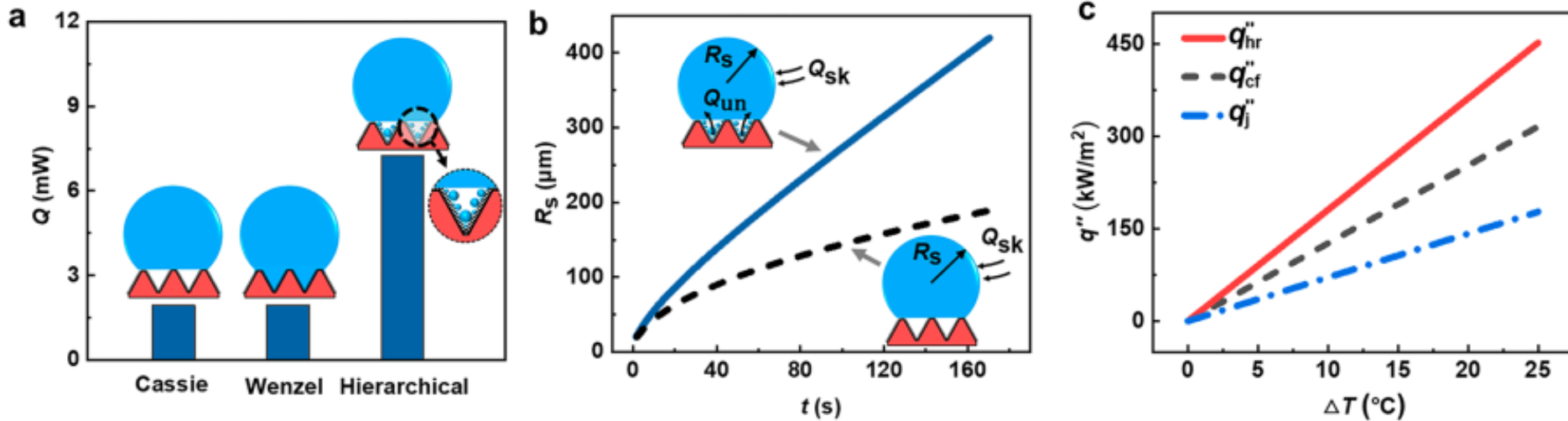
(a) Droplet diameter ( $2R$ ) as a function of time ( $t$ ) (b) Droplet diameter as a function of time for droplets growing underneath CB sink droplets at different cavity depth locations. The droplets analyzed were small enough so that droplet growth was primarily driven by direct vapor condensation. Droplet size distribution of the underlying droplets at the (c) upper focal plane near the hilltop regions and (d) lower focal plane near the bottom, with respect to the projected area. Error bars in (a) and (b) represent one standard deviation of three independent measurements of the droplet diameters. Error bars in (c) and (d) represent one standard deviation of droplet number counts in three consecutive frames spanning 10 min of condensation. Data collection was performed 10 min after condensation initiated to ensure quasi-steady-state conditions. Note, due to optical microscopy limitations in spatial resolution, droplets having  $2R < 1.5 \mu\text{m}$  are not shown in (c) and (d).

# Overall surface condensation heat transfer



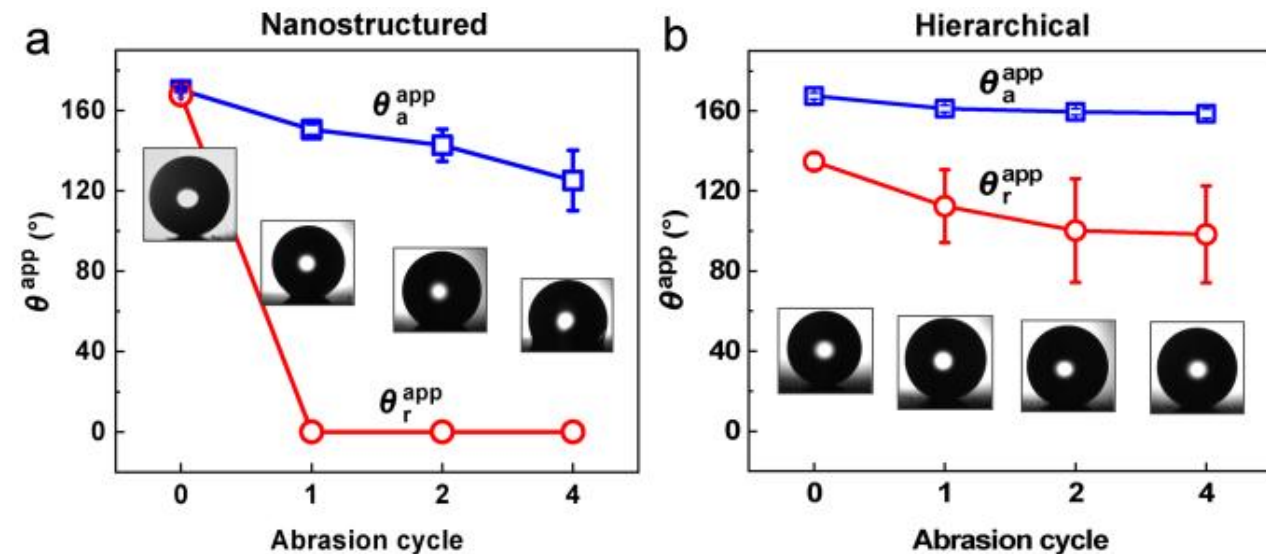
(a) Schematic showing the temperature drop through the CB sink droplet and identifying the vapor velocity entering the cavities beneath the droplet. Vapor depletion due to condensation beneath the sink droplet introduces a net vapor flow with velocity  $v_c$  entering the microcavities. (b) Droplet base temperature,  $T_b$ , as a function of sink droplet radius  $R_s$ . (c) Top-view schematic showing  $v_c$  entering the underlying cavities. (d) Vapor velocity,  $v_c$ , as a function of  $R_s$ . As a comparison, we also plot the velocity toward the condensing surface without sink droplets ( $v_0$ ). Note that  $v_c$  is parallel to the substrate, while  $v_0$  is perpendicular. Model parameters: vapor saturation temperature  $T_v = 25$  °C, substrate temperature  $T_c = 5$  °C,  $q_0'' = 0.1$  W/cm<sup>2</sup>,  $\theta_{app} = 150^\circ$ , flat-topped square micropyramid spacing/top width/height  $s_m/d_m/h_m = 50/10/40$  μm, nanostructure  $s_n/d_n/h_n = 0.5/0.12/1$  μm.

# Overall surface condensation heat transfer

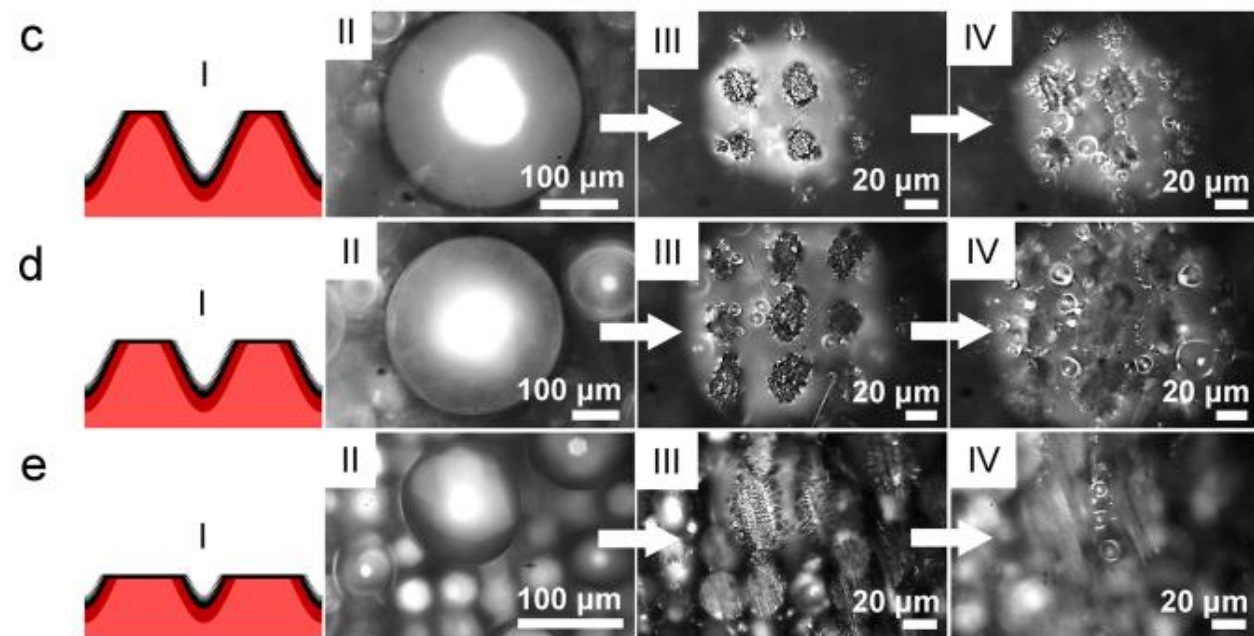


(a) Heat transfer ( $Q$ ) through an individual droplet in differing configurations: CB state, Wenzel state, and hierarchical mode (CB sink droplet with shaded droplets). (b) Droplet radius ( $R_s$ ) of an individual sink droplet with and without shaded droplets as a function of time ( $t$ ). (c) Heat fluxes ( $q''$ ) of hierarchical condensation ( $q''_{hr}$ ), condensation devoid of shaded droplets ( $q''_{cf}$ ), and jumping-droplet condensation ( $q''_j$ ) as a function of surface subcooling ( $\Delta T$ ). Model parameters:  $T_v = 25$   $^{\circ}\text{C}$ ,  $\theta_{a\text{ app}} = 150^{\circ}$ , nucleation site density  $N_s = 2.5 \times 10^9 \text{ m}^{-2}$ ,  $sm/hm/dm = 50/40/10$   $\mu\text{m}$ ,  $sn/dn/hn = 0.5/0.12/1$   $\mu\text{m}$ . In (a) and (b),  $\Delta T = 5$   $^{\circ}\text{C}$ ,  $R_s = 300$   $\mu\text{m}$ ; in (c),  $\Delta T$  was varied with  $T_v = 25$   $^{\circ}\text{C}$ , and maximum sink droplet radius  $R_g = 500$   $\mu\text{m}$ .

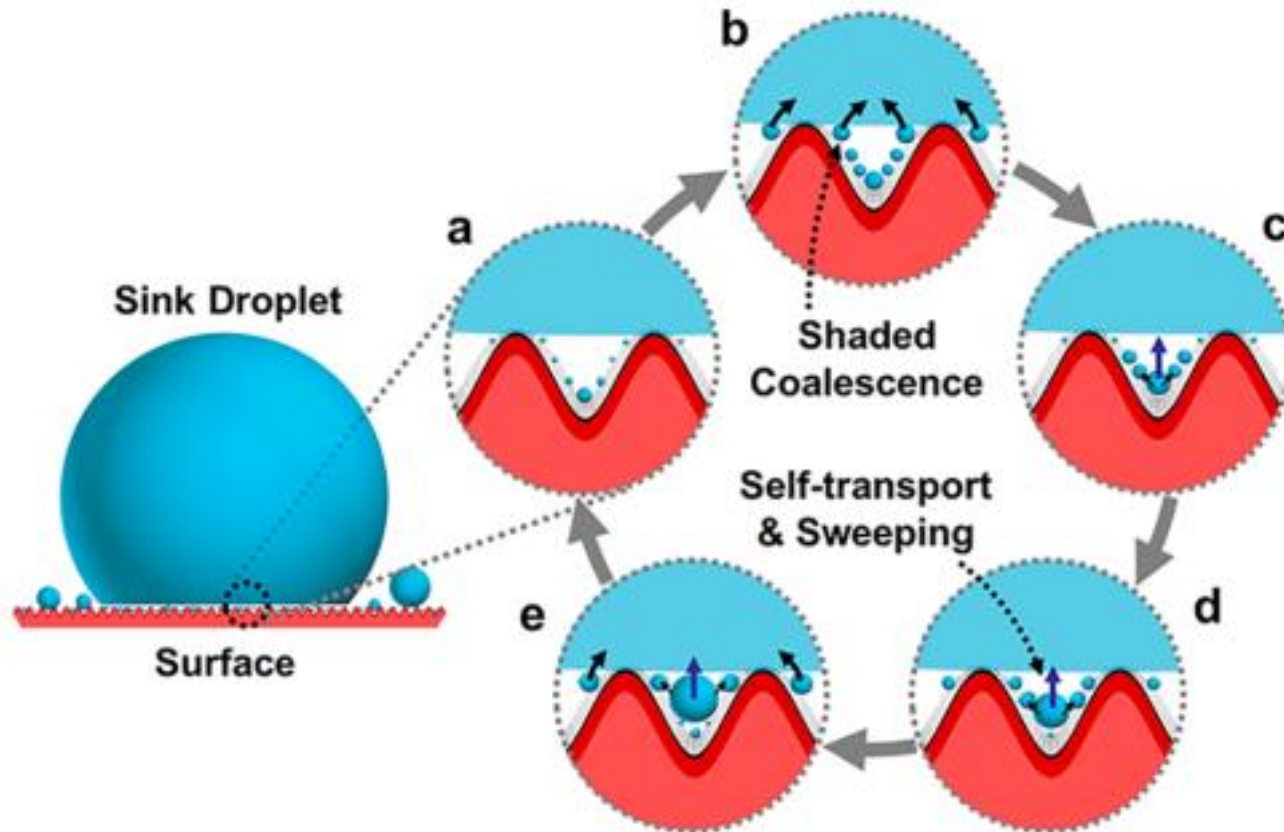
# Durability to abrasive wear



Apparent advancing ( $\theta_a^{app}$ ) and receding ( $\theta_r^{app}$ ) contact angles as a function of abrasive wear test cycles for the (a) single-tier CuO nanoblade surface and (b) hierarchical CuO nanoblade surface. Droplet radius is  $\sim 200 \mu\text{m}$ . (c-e) Hierarchical condensation on the hierarchical CuO nanoblade surfaces with increasing extents of abrasive damage. The extent of microstructure damage is schematically shown in (c-I), (d-I), and (e-I), with microstructures in (c) being slightly damaged, while in (e) drastically abraded. Sink droplets on the abraded surfaces are shown in (c-II), (d-II), and (e-II), respectively.

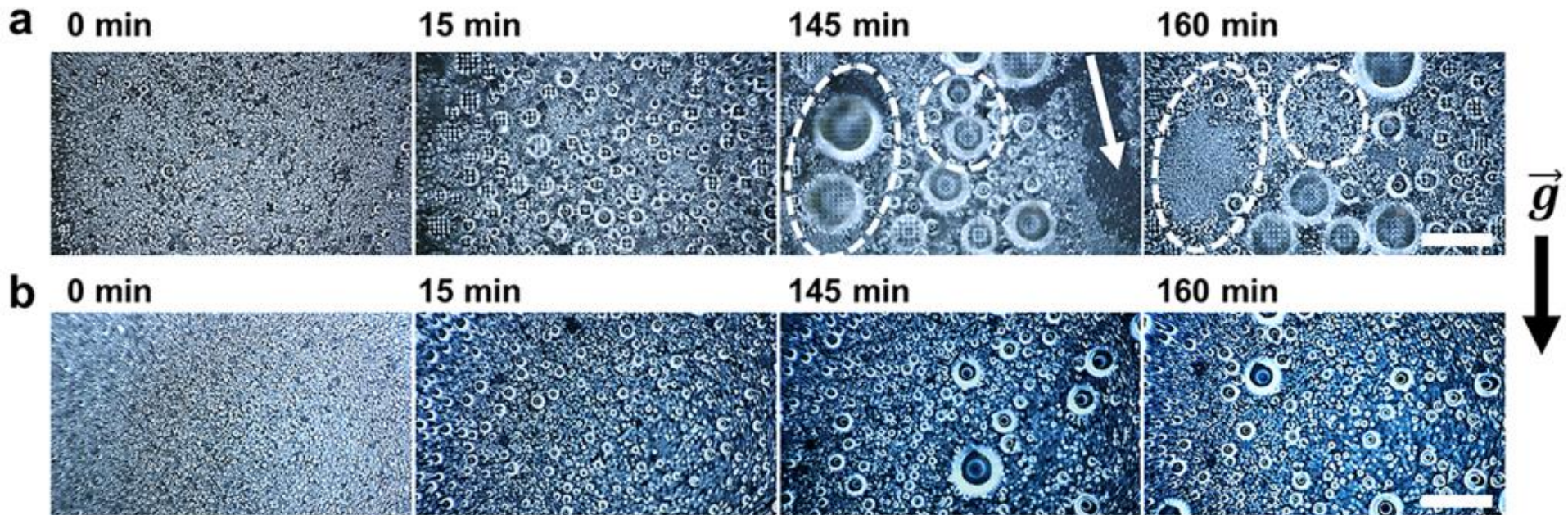


# Surface structure design guidelines



Schematic of stable hierarchical condensation. During condensation, small shaded droplets near the hilltop regions (a) nucleate and grow beneath CB sink droplets until they (b) touch the liquid-vapor interface at the base of the sink droplet and are sucked into the sink droplet, after which (c) re-nucleation and growth of new generations of droplets at the same sites occur. Meanwhile, (d) the growing droplets at the bottom of the microscale valleys climb upward spontaneously along the divergent microcavities with the aid of droplet coalescence and capillary forces, until they (e) reach the sink droplet and coalesce with it, enabling (a) surface clearing and re-nucleation. Once large enough to be removed by gravity, the sink droplet is removed from the surface and the cycle initiates again. On a rationally designed micro/nanostructured surface, the hierarchical condensation cycle can proceed sustainably.

# Testing hierarchical condensation efficiency



Optical images of condensation, coalescence, and shedding of droplets on a vertically oriented (a) hierarchical CuO nanoblade surface and (b) single-tier CuO nanoblade surface. Coalescence-induced jumping of millimeter-scale droplets is identified by the white-dotted circles, and the track of gravitation-induced droplet shedding is identified by the white arrow. Scale bars: 1 mm.

**THANK YOU**